UNSTABLE PHENOMENON OF FLOW IN A MIXING VESSEL WITH A MARINE PROPELLER

SUGENG WINARDI AND YOICHI NAGASE
Department of Chemical Engineering, Hiroshima University, Higashi-Hiroshima 724

Key Words: Mixing, Marine Propeller, Unstable Phenomenon, Visualization, LDV, Flow Profile

Unstable flow phenomena in a mixing vessel with a marine propeller were investigated experimentally using flow visualization and LDV techniques. It was found that the instantaneous bulk flow profiles were usually asymmetric with respect to the impeller shaft and they fluctuated in the large time scale. The circulation flow patterns in the space between two adjacent baffles were classified into quick-return flow (QR), full-circulation flow (FC) and intermediate-circulation flow (IC), which were replaced randomly one after another with time. Their lifetimes were widely distributed from about half a second to several minutes. Connected with the circulation flow patterns, the impeller stream was directed vertically downward or obliquely outward to the vessel wall and held a high level of angular momentum when pattern FC took place, while the impeller stream was directed obliquely inward to the impeller shaft with a low level of angular momentum when pattern QR took pace.

Introduction

Hydrodynamic studies of mixing vessels have been extensively developed since 1960 for the problems of flow profile in the vessel, impeller pumping capacity, impeller efficiency, turbulent characteristics of the flow and so on. However, most researchers used the disc turbine or pitched (inclined) blade turbine.[1-7,9,10,13-18,20,21] A few studies have been carried out for the fan turbine (paddle) or propeller.[8,11,12,15,17-19]

Concerning turbulent measurement of the flow in a mixing vessel, the question is that why turbulent intensities within most of the vessel are of high level. In connection with this problem, the authors[17] have recognized that when a fan turbine was used the flow in the mixing vessel fluctuated unstably in vessel scale and in the large time scale (several seconds or less). That is, if the flow field in the vessel was divided into observations of one or several seconds duration, the flow profiles within those intervals were considerably different from one another. They were replaced one after another with time. Also, the instantaneous bulk flow profile was asymmetric with respect to the impeller shaft. A similar phenomenon was reported by Oldshue.[12]

It is well known that the marine propeller is an impeller with low power consumption per unit circulation flow rate, thus producing a circulation flow with low turbulent level compared with those produced by the disc turbine, fan turbine and inclined-blade turbine. It is interesting to investigate whether the flow phenomena in a mixing vessel with a marine propeller are also unstable in the sense similar to those produced by a fan turbine as mentioned above, since it is estimated that such unstable flow phenomena could have a significant role in large-scale mixing. To achieve this objective, investigations were carried out experimentally using flow visualization and LDV techniques.

1. Experimental work

Dimensions of the vessel are shown in **Fig. 1**. The vessel was a transparent acrylic resin cylindrical tank with flat bottom. A circular shape was almost

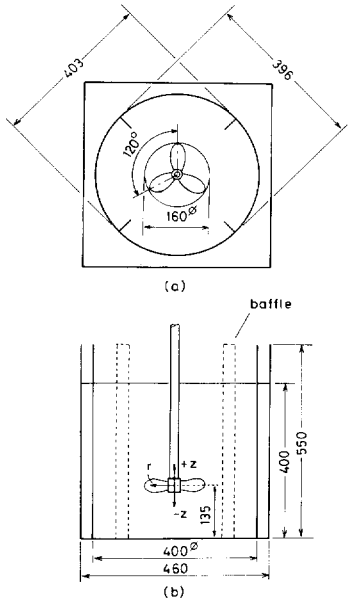

Fig. 1. Experimental apparatus and coordinate system

* Received August 31, 1990. Correspondence concerning this article should be addressed to S. Winardi.

maintained in the vicinity of the vessel bottom since it was inserted into a circular groove in the bottom plate. A slight distortion from the circular shape was found at the vessel top; that is, at a height of 550 mm from the bottom the vessel shape was approximately ellipsoidal with diameters of 403 and 396 mm along the long and short axes respectively, as depicted in Fig. 1(a). Four baffles were mounted symmetrically along the long and the short principle axes of the vessel top, as shown in the figure. The impeller shaft was aligned and placed coincidently with the center line of the vessel. Filled with water as the working fluid to a height of 400 mm, the vessel was placed in a square glass tank which was also filled with water to minimize optical distortion.

A three-blade commercial marine propeller was used. Its symmetry was examined and modified. The blade cross section was shaped to be similar to that of a wing. Details of the dimensions and geometry of the impeller are shown in **Fig. 2**. The impeller was rotated at a constant speed of 3 rps, which corresponds to a Reynolds number of 4.8×10^4.

Polystyrene particles of approximately 0.5 mm in diameter were used as tracer for flow visualization. Human, high-speed VTR and camera observations were used for visualization. Human observations were carried out by four observers who were positioned to observe the circulation flow patterns simultaneously near the vessel wall in each space between two adjacent baffles. A high-speed VTR or a stationary camera was used for observing the side view of the overall flow field in the vessel or the impeller stream. The camera was operated at a shutter speed of 1/8 second. Velocity measurement of the impeller stream was made with an LDV equipped with a frequency shifter.

2. Results and Discussion

2.1 Circulation flow

Instability and pattern recognition The unstable flow phenomena in the vessel with propeller was easier to recognize by looking at the circulation flow rather than at the impeller stream. From simultaneous observations of the circulation flow using a high-speed VTR and the four observers, the unstable flow phenomena could be classified approximately into the following patterns.

The impeller stream turns upward as it approaches the vessel wall. When observation was focused on the bulk motion of tracer particles within each baffle space, it was found that the upward flow from the bottom returns quickly into the impeller region as a whole near the height of the impeller intermittently for a certain time interval. This flow is denoted as quick-return flow (pattern QR) hereinafter.

However, the impeller stream that reaches the other baffle space turns to ascend along the vessel wall

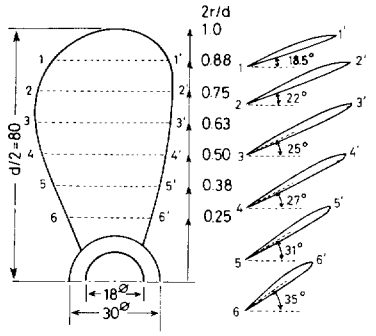

Fig. 2. Dimensions and geometry of a marine propeller

toward the liquid surface. A part of this flow returns directly into the impeller region on the way. Near the liquid surface, the other part turns and streams across the impeller shaft toward the baffle spaces where the pattern QR takes place, and no part of it turns downward along the shaft into the impeller region. Near the vessel wall, this part turns downward and streams along the vessel wall to collide with the pattern QR. Then they return together into the impeller region. This flow is denoted as full-circulation flow (pattern FC).

The difference of patterns QR and FC could be easily identified from stereoscopic observation. Because the flow is complicated, besides patterns QR and FC there are many possibilities of circulation flows that are difficult to classity into pattern QR or FC. They are identified as intermediate-circulation flows (pattern IC).

These patterns, of course, are not well defined but are roughly recognized patterns which were first obtained from continuous and stereoscopic observations. Therefore, it is difficult to confirm them from the many pictures. **Figure 3(a)** is a sample picture of the side-view of the flow profile in the middle plane between two baffles, where the patterns QR and FC take place in the right-hand and left-hand sides of the figure respectively. **Figure 4(a)** shows the condition opposite to that of the Fig. 3(a).*)

From visualization, it can be recognised that symmetric circulation flow with respect to the impeller shaft was not often found. The instantaneous flow profiles in the overall vessel were usually axi-asymmetric.

Pattern lifetime distribution It is noted that the four baffle spaces were usually occupied by various

*) Note the flow in the lower part or in the upper part of the vessel. The flow is remarkably three-dimensional in the upper part, so that the tracer particles, which enter or leave the light plane, increase in number. Consequently, it is difficult to obtain the image of the flow from these figures alone. Arrows are therefore shown in Figs. 3(a) and 4(a) to indicate the flow directions (not the velocity vector representations). Each figure was obtained by projecting the tracer particle trajectories from a photograph.

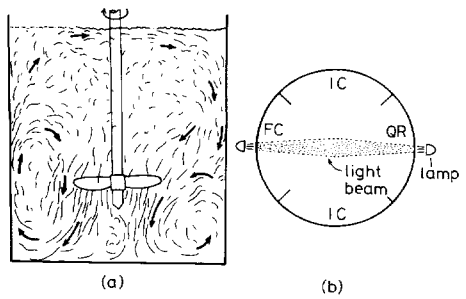

Fig. 3. Illustration of instantaneous circulation flow profile-case 1. Arrows indicate the direction of flow

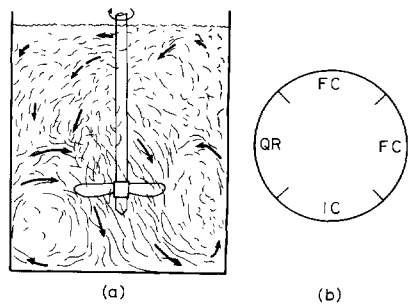

Fig. 4. Illustration of instantaneous circulation flow profile-case 2

combinations of the patterns QR, IC and FC. The generation of each pattern was random in space and time.

It is interesting to see the lifetime of each flow pattern and their combinations which appeared simultaneously in the four baffle spaces. Measurement of the pattern lifetimes was made by the human observations described above. Observations were continuously carried out for one hour. The following results were obtained, although they may include personal errors.

The lifetime distribution of each pattern appearing in the four baffle spaces is given in **Figs. 5, 6 and 7** for patterns QR, FC and IC respectively. The abscissa in these figures is non-dimensionalized by one rotation time of the impeller, which was one-third of a second in these experiments. As seen in these figures, the lifetime of each pattern is widely distributed, but is usually short as it is seen that the peak value of each figure occurs at 2 to 6 seconds of the lifetime. However, a certain pattern with a long lifetime sometimes appeared intermittently in one of the baffle spaces. Actually, any one of the four baffle spaces was usually occupied by pattern QR, IC or FC for ten and several seconds or more. The other baffle spaces were occupied by patterns having short lifetimes. Sometimes two baffle spaces were occupied by patterns with longer lifetime. The same or different patterns appeared randomly for a short lifetime in two or three other baffle spaces. These results indicate that the lifetime of a pattern combination in the vessel is short as a whole.

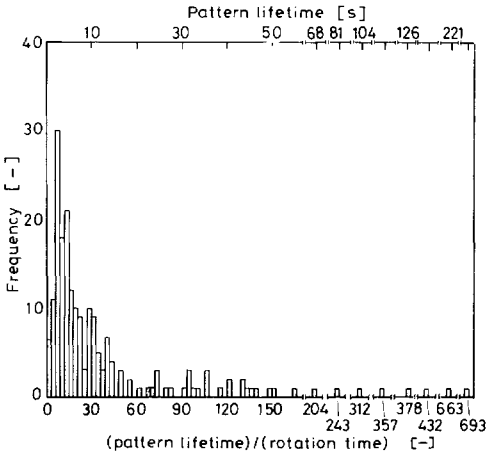

Fig. 5. Lifetime distribution of pattern QR; average lifetime = 16.1 seconds

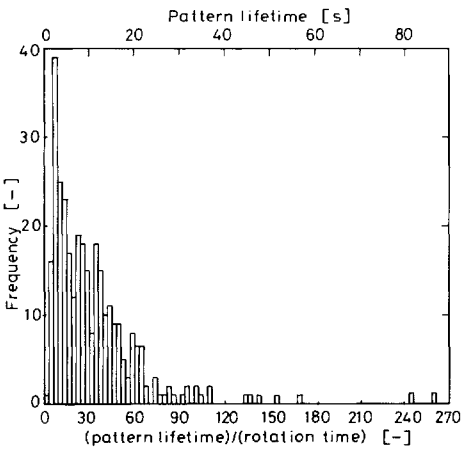

Fig. 6. Lifetime distribution of pattern FC; average lifetime = 11.4 seconds

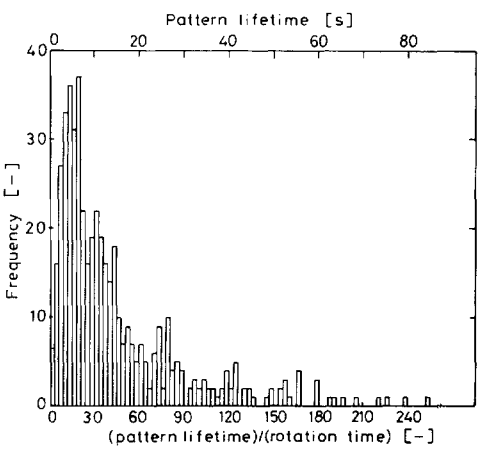

Fig. 7. Lifetime distribution of pattern IC; average lifetime = 15.7 seconds

Lifetime and frequency of the pattern combinations when four baffle spaces were observed clockwise (the same direction as the impeller rotation), are shown in **Table 1**. The frequency of the pattern combination

Table 1. Frequency of pattern combinations in the vessel

Pattern combination	Frequency [%]	Average lifetime [s]
QR-IC-QR-IC	0.7	2.6
QR-IC-QR-FC	1.1	2.9
QR-QR-IC-IC	5.0	3.5
QR-QR-IC-FC QR-QR-FC-IC	7.6	3.9
QR-IC-IC-IC	14.7	4.3
QR-IC-IC-FC FC-IC-IC-QR	16.1	5.6
QR-IC-FC-IC	11.6	4.0
QR-IC-FC-FC IC-QR-FC-FC	8.9	3.8
QR-FC-IC-FC	5.5	4.9
QR-FC-FC-FC	3.1	4.0
IC-IC-IC-IC	6.0	4.0
IC-IC-IC-IC	11.6	4.0
IC-IC-FC-FC	3.7	3.1
IC-FC-IC-FC	1.3	3.5
Others	3.1	2.3

QR-IC-IC-IC, QR-IC-IC-FC, QR-IC-FC-IC or IC-IC-IC-FC is relatively high. Their sum is more than 54%. Results in Table 1 demonstrate again that most of the pattern combinations were asymmetric. Pattern combinations which do not include QR, IC or FC are 23.3%, 4.4% and 27.5% respectively. Thus pattern IC usually occurs simultaneously with the other patterns in one or more baffle spaces. The average lifetimes of the pattern combinations are distributed in the narrow range of 2 to 5.6 seconds.

2.2 Impeller stream

Flow visualization Since the unstable flow phenomena of the impeller stream could hardly be recognized, as mentioned above, the impeller stream was observed as to how it changes when pattern QR or FC is taking place in the baffle space. It was also interesting to ask whether a highly coherent flow like a trailing vortex generated behind the blade of a disc turbine or fan turbine could also be found with the propeller. Here observation was focused on taking close-up photographs of the impeller stream, using a stationary camera. As shown in **Fig. 8**, a slit beam of continuous light was introduced obliquely upward from the vessel bottom to the impeller region and a strobo-flash was used simultaneously to confirm the instantaneous blade position. The pictures were taken when baffle space A in the figure was occupied by either pattern QR or FC. Illustrations of the impeller stream, when patterns QR and FC are taking place, are given in **Figs. 9** and **10** respectively. The figures indicate that most of the particle trajectories are in the range of $r=(0.5\sim0.8)d/2$, that is, in the vicinity of the maximum blade width. When pattern QR is taking place, the impeller stream is usually directed obliquely inward to the impeller shaft ($u_r<0$), but the impeller

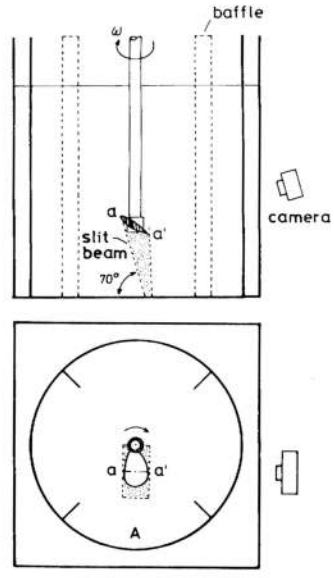

Fig. 8. Lighting system and camera arrangement for flow visualization of the impeller stream

Fig. 9. Illustration of impeller stream when pattern QR is taking place

Fig. 10. Illustration of impeller stream when pattern FC is taking place

stream flows vertically downward or obliquely outward to the vessel wall ($u_r\geqslant0$) when pattern FC is taking place. As indicated by arrows A and B in these figures, a small-scale trailing vortex near the blade tip and a steady vortical motion in the region between the tip of the impeller shaft and the vessel

bottom are found. A trailing vortex is generated intermittently when either pattern QR or FC is taking place. It is seen that the blade edge of similar shape to that of a wing could produce a small-scale trailing vortex.[18] The vortical motion in the region below the impeller shaft moves downward very slowly with a low rotational velocity. Therefore, it is estimated that the vorticity and the energy transferred by these vortices are also small.

Detailed measurement of the impeller stream To confirm quantitatively the difference between the impeller stream characteristics when pattern QR or FC is taking place, velocity measurements by LDV were attempted for the impeller stream just below the impeller. Then the visualization of the flow in the baffle spaces was performed simultaneously with the velocity measurements. To observe the circulation flow pattern in the baffle space, three streamers were placed vertically, close to the vessel wall at three heights from the vessel bottom in each of the middle planes between two baffles. Consequently, this measurement could identify approximately the circulation flow pattern that appeared in the baffle space of pattern QR or FC. Velocity measurement was made when pattern QR or FC was taking place. Judgement of the flow pattern in this measurement was more uncertain than that by the previous visualization method. However, it is believed that the results given as follows are useful. Since the lifetime of pattern QR or FC was short, as mentioned above (see Figs. 5, 6 and 7), each velocity measurement was conducted for three seconds and the data were accumulated for forty-five seconds of the total time, which was equivalent to 30,000 data for pattern QR or FC. Measurements were made on the horizontal plane 5 mm below the lower edge of the maximum blade width at various radial distances from the impeller axis.

Radial distributions of the ensemble average velocities and turbulent intensities normalized by the impeller tip velocity, $(d/2)\omega$, are shown in **Figs. 11, 12** and **13** for axial, radial and tangential components respectively.

Figure 11 indicates that there is no significant difference between the $\bar{u}_z$ distributions when patterns QR and FC are taking place. The maximum values of $\bar{u}_z$ are found in the vicinity of maximum blade width. This result approximately confirms the high-speed flow observed in the visualization. It can be seen that $|\bar{u}_z|$ increases at first to reach a maximum at $2r/d=0.75$, then decreases sharply with increasing radial distance from the impeller shaft. The positive signs of u_z in the range of $2r/d>1.8$ indicate upward flow near the vessel wall. For comparison, the data from previous works[8,11,19] are plotted in Fig. 11. Further discussion cannot to given here, since the

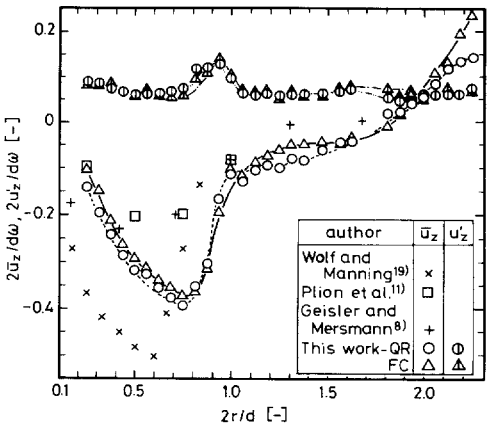

Fig. 11. Radial distributions of $\bar{u}_z$ and u'_z at $z=-20$ mm

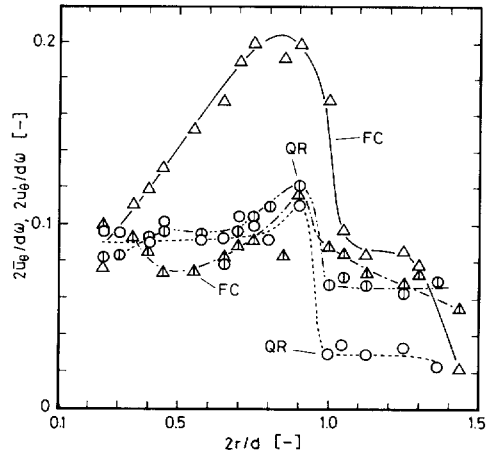

Fig. 12. Radial distributions of $\bar{u}_r$ (○, △) and u'_r (◑, ◭) at $z=-20$ mm

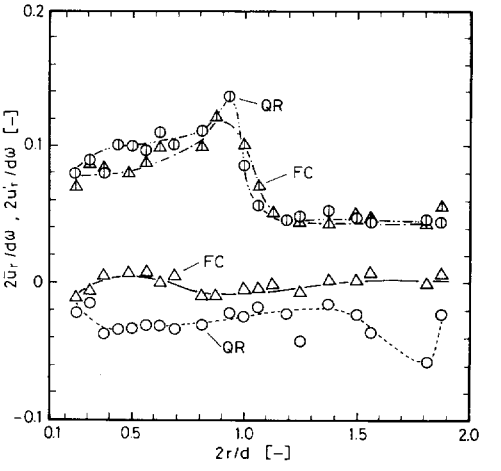

Fig. 13. Radial distributions of $\bar{u}_\theta$ (○, △) and u'_θ (◑, ◭) at $z=-20$ mm

geometry and pitch specifications of the propellers were not presented in those papers. The values of u'_z distributions when patterns QR and FC take place are nearly equal, with less variation over the measurement range except in the narrow region of $2r/d=0.95\sim1$, where small peaks of the distributions

are found.

As shown in Fig. 12, the $\bar{u}_r$ distribution is nearly zero over the measurement range when pattern FC is taking place. This indicates that the impeller stream flows vertically downward. However, the $\bar{u}_r$ distribution has a negative velocity when pattern QR is taking place. This reveals a flow which streams obliquely inward to the impeller shaft. These results are in agreement with those of the visualization. The values of u'_z when patterns QR and FC take place are also equal over the measurement range, with peaks that lie in the blade-tip region.

It is noted that when pattern FC is taking place in the baffle space, the $\bar{u}_\theta$ distribution is remarkably different from that when pattern QR is taking place, as shown in Fig. 13. For pattern FC, large values of $\bar{u}_\theta$ are found in the impeller stream. Then they decrease sharply from the blade tip with increasing radial distance. For pattern QR, relatively small values of $\bar{u}_\theta$, approximately half of those when pattern FC is taking place, are found over the measurement range. It can be said that when pattern FC is taking place, the angular momentum ($=\rho r^2 \bar{u}_z \bar{u}_\theta$) transferred is much larger than that when pattern QR is taking place. Consequently, it is estimated that the impeller stream for pattern FC can circulate to rise up to the liquid surface. The maximum values of u'_θ also appear in the blade-tip region similar to those appearing in the u'_z and u'_r distributions. This may be caused by the presence of the trailing vortex near the blade tip. Almost equal magnitude of turbulence intensities among the three components of velocity is observed in the impeller stream.

Figure 14 illustrates the velocity fluctuation near the lower edge at maximum blade width ($2r/d=0.69$) when pattern FC is taking place. Sharp peaks of velocity fluctuations often appear at every blade passage for each component of velocity. This indicates that only the fluid close to the impeller blade is highly accelerated, especially in the radial and tangential directions. The discharge stream is relatively gentle in the middle region between blades but is strong and violent only in the vicinity of the blade.

Conclusions

It was confirmed that, even when a marine propeller whose power number is less than that of the fan turbine was used, the circulation flow in the mixing vessel fluctuated in the vessel scale and large time scale. The instantaneous circulation flow profiles in the vessel scale were usually asymmetric about the impeller shaft. The circulation flow patterns in the baffle spaces were classified into quick-return flow (pattern QR), full-circulation flow (pattern FC), and intermediate-circulation flow (pattern IC). They were replaced randomly one after another. Their lifetimes were

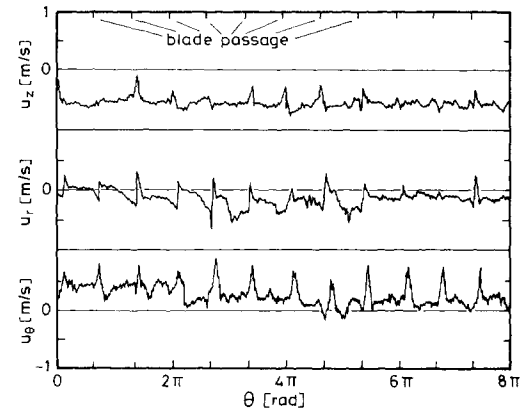

Fig. 14. Illustration of instantaneous velocity trace at $r=55$ mm, $z=-20$ mm

distributed from about half a second to several minutes. A certain pattern combination appeared for several seconds and then changed to another pattern combination randomly.

The impeller stream would change as a result of the change in these patterns. The impeller stream was directed obliquely outward to the vessel wall or vertically downward when pattern FC took place in the baffle space, and obliquely inward to the impeller shaft when pattern QR took place. A large difference in the $\bar{u}_\theta$ distributions between patterns FC and QR was found. Thus when pattern FC taking place the angular momentum transferred was much larger than that when pattern QR was taking place. Finally, it can be concluded that the impeller stream is significantly affected by the unstable phenomena of the circulation flow profile.

Nomenclature

d	=	impeller diameter	[m]
r	=	radial distance from impeller shaft	[m]
$\bar{u}_r, \bar{u}_\theta, \bar{u}_z$	=	radial, tangential and axial ensemble average velocities	[m/s]
u'_r, u'_θ, u'_z	=	radial, tangential and axial turbulent intensities	[m/s]
z	=	axial distance from impeller center	[m]
ω	=	angular velocity of impeller	[s^{-1}]

Literature Cited

1) Armstrong, S. G. and S. Ruszkowski: *Proc. 6th European Conf. on Mixing*, Pavia, Italy, 1988. pp. 1–14.
2) Bujalski, W., A. W. Nienow, S. Chatwin and M. Cooke: *Chem. Eng. Sci.*, **42**, 317 (1987).
3) Calabrese, R. V. and C. M. Stoot: *Chem. Eng. Prog.*, **85**, 43 (1989).
4) Chang, T. P. K., A. T. Watson and G. B. Tatterson: *Chem. Eng. Sci.*, **40**, 269 (1985).
5) Chen, K. Y., J. C. Hajduk and J. W. Johnson: *Chem. Eng. Commun.*, **72**, 141 (1988).
6) Costes, J. and J. P. Couderc: *Chem. Eng. Sci.*, **43**, 2751 (1988).
7) Fort, I.: *in Mixing-Theory and practice* edited by Uhl, V. W and J. B. Gray. Academic Press, New York, 1986.

8) Geisler, R. K. and A. B. Mersmann: *Proc. 6th European Conf. on Mixing*, Pavia, Italy, 1988. pp. 267–272.
9) Klaboch, L., M. Patcnik, J. Lamka and I. Fort: *Proc. 6th European Conf. on Mixing*, Pavia, Italy, 1988. pp. 35–42.
10) Laufhutte, H. D. and A. B. Mersmann: *Ger. Chem. Eng.*, **8**, 371 (1985).
11) Plion, P., J. Costes and J. P. Couderc: *Proc. 5th European Conf. on Mixing*, Wurzburg, F. R. Germany, 1985. pp. 341–353.
12) Oldshue, J. Y.: *Fluid Mixing Technology*. Chem. Eng. McGraw-Hill Pub., 1983.
13) Ranade, V. V. and J. B. Joshi: *Chem. Eng. Comm.*, **81**, 197 (1989).
14) Ranade, V. V. and J. B. Joshi: *Trans. Instn Chem. Engrs.*, **68**, 19 (1990).
15) Sano, Y. and H. Usui: *J. Chem. Eng. Japan*, **18**, 47 (1985).
16) Tsurusaki, H. and T. Urata: *Nihon Kikai Gakai Ronbunshu*, **55**, 2318 (1989).
17) Winardi, S., S. Nakao and Y. Nagase: *J. Chem. Eng. Japan*, **21**, 503 (1988).
18) Winardi, S., M. Kuwai and Y. Nagase: *Mem. Fac. Eng., Hiroshima Univ.*, **10**, 37 (1990).
19) Wolf, D. and F. S. Manning: *Can. J. Chem. Eng.*, **44**, 137 (1966).
20) Wu, H. and G. K. Patterson: *Chem. Eng. Sci.*, **44**, 2207 (1989).
21) Yianneskis, M., Z. Popiolek and J. H. Whitelaw: *J. Fluid Mech.*, **175**, 537 (1987).